Northeastern University
Architecture for Extracting Groundwater In Regolith (AEGIR)

RASC-AL 2022: Mars Water-based ISRU Architecture

Team Members:

Eddie Berman - Undergraduate Physics and Mathematics Major
Harrison Burke - Undergraduate Mechanical Engineering Major
Cameron Castonguay - BS/MS Biomechanical Engineering Major
Javier Coindreau - Undergraduate Computer Engineering Major
Meghan Gallagher - BS/MS Biomechanical Engineering Major
Andrew Han - Undergraduate Mechanical Engineering Major
Spencer Karrat - Undergraduate Computer Science Major
Matt Longtin - Undergraduate Physics and Chemical Engineering Major
Lee Milburn - Undergraduate Computer Engineering Major
Ryan Norris - Undergraduate Mechanical Engineering Major
Lindsay Riggs - Undergraduate Computer Science Major
Aidan Tillman - Undergraduate Bioengineering Major

Advised by:
Professor Taskin Padir, Ph.D

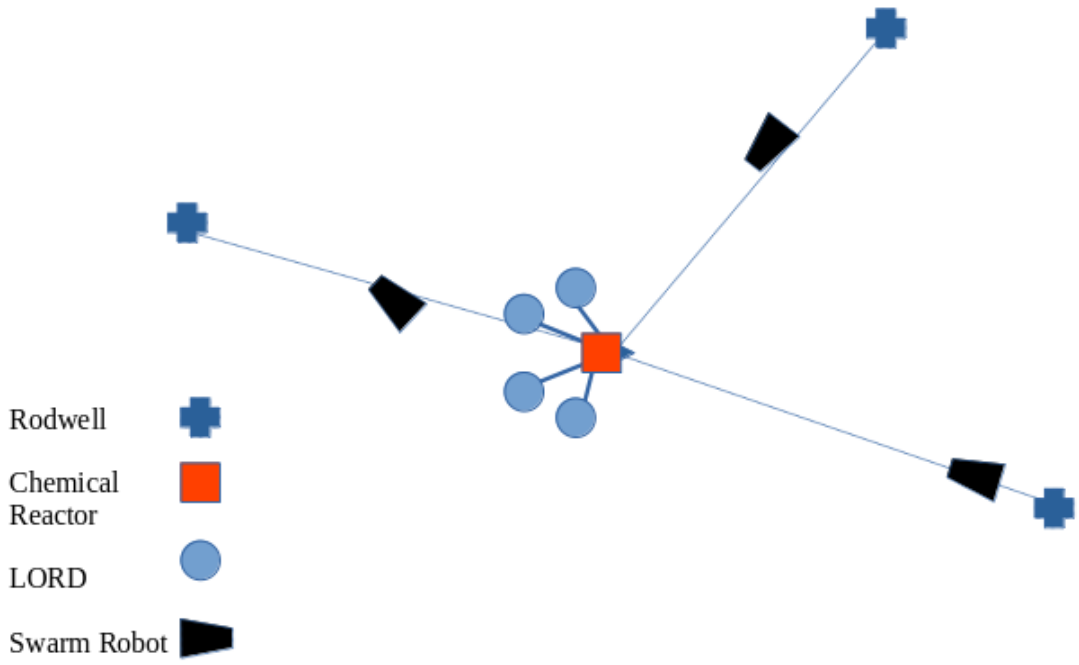

Northeastern University: Architecture for Extracting Groundwater In Regolith (AEGIR)

Theme: Mars Water-based ISRU Architecture

Objectives & Technical Approach:

- Aims to construct an ISRU systems on Mars that converts water into propellant
- Consists of four systems:
  - Modified Rodriguez wells for water acquisition
  - Autonomous robots for water transport
  - Conversion system (electrolysis and Sabatier)
  - Liquid Origami Rigidized Drum (LORD) cryogenic tanks for propellant storage

Image:

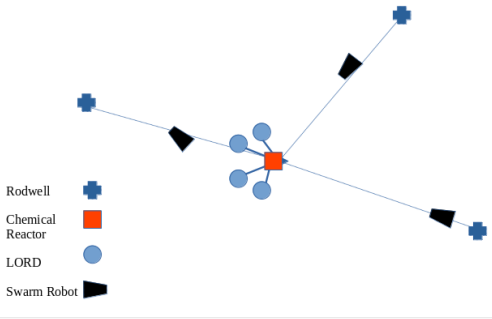

Key Design Details & Innovations:

- Total mass: 42.3 t
- Usage of RTGs and solar panels for optimization of power input
- Combined water electrolysis and Sabatier reactor for more efficient conversion rates
- Autonomous robotic transport and acquisition system
- Liquid Origami Rigidized Drum (LORD) systems allows inflatable vessels to expand at cryogenic temperatures without experiencing microcracking
  - Greatly improves packing efficiency for the tanks en route to Mars

Schedule:

- System Development Start: 2030Q3
- System Fabrication & Testing: 2032Q2
- System Launch: 2034Q4
- Deployment on Martian Surface: 2035Q3
- Drills Fully Operational: 2035Q4

Cost:

- Total proposed budget $6.61 billion.

1. Mission Overview

1.1 Introduction

The Architecture for Extracting Groundwater In Regolith (AEGIR) is a proposed design for a full-scale mission architecture to establish a system for in-situ resource utilization (ISRU) on the Martian surface. By using resources found on Mars, space travel can expand farther from Earth than previously possible. AEGIR specifically will use Martian water reserves to produce cryogenically stored methalox propellant that can be used to refuel spacecraft on Mars, therefore reducing the overall mass of said spacecraft. This mission has a technology readiness and launch target of 2034Q4 to utilize Mars' close approach in 2035Q3. This proposal will give an overview of the overall mission architecture and the designs for the four systems, including cost and risk analyses based upon current technological analogs.

1.2 Background

As space travel develops and expands, it will be necessary for NASA to have the ability to produce important materials such as crew consumables and propellant with materials found beyond the Earth using ISRU. NASA is currently developing technology to locate and utilize these materials, including VIPER, a mobile robot investigating the lunar South Pole, that is the first resource mapping mission beyond Earth and there is current research towards developing an ISRU system for use on the Moon that will also serve as a testbed for ISRU on Mars [1].

1.3 Purpose and Objectives

AEGIR is a system designed to acquire water found below the surface of Mars, convert it into fuel and oxidizer, then store the propellant cryogenically for use by ascent vehicles. Its primary objective is to reduce the upmass of spacecraft traveling to Mars. Currently, transports carry the fuel necessary for the trip, increasing the mass of the payload. Increased mass, in turn, increases cost and risk and decreases the available space on the vehicle, infringing upon mission goals and reducing the capability for space exploration and analysis. This complicates both human missions and robotic sample return.

By decreasing the upmass of a system, the main goal of AEGIR, NASA spacecraft will have the capability to increase supplies for the crew, scientific instrumentation, and space for scientific samples. Additionally, if ISRU systems are extending throughout the solar system, spaceflight duration can extend, allowing for much greater exploration and flexibility.

1.4 Mission Concept

AEGIR is a fully autonomous ISRU architecture that uses Martian water to produce cryogenic propellant. The first stage of AEGIR is to acquire water from underground reserves using modified Rodriguez wells. The mission lands in the Arcadia Planitia as it houses large deposits of ice and has flatter terrain, making it more friendly to the robots' and drills' mobility [2]. This water is then transported by a trio of automated robots to a central chemical reactor to convert water and carbon dioxide from the atmosphere into oxygen and methane. Once processed, the cryogens are stored in Liquid Origami Rigidized Drum (LORD) systems, which involve the use of origami to allow inflatable vessels to expand at cryogenic temperatures without experiencing microcracking. The use of inflatable tanks greatly improves packing efficiency for the tanks en route to Mars. Packing efficiency is a major issue for storage in space travel and this system relies on recent research to mitigate that problem.

1.5 Project Timeline

Jet Propulsion Laboratory will manage this mission due to the extensive use of robotic operations. Development of AEGIR is expected to begin in 2030 due to the materials science research needed and will launch in time for the 2034 Mars transfer window. The core mission is expected to last 5 years, through 2040.

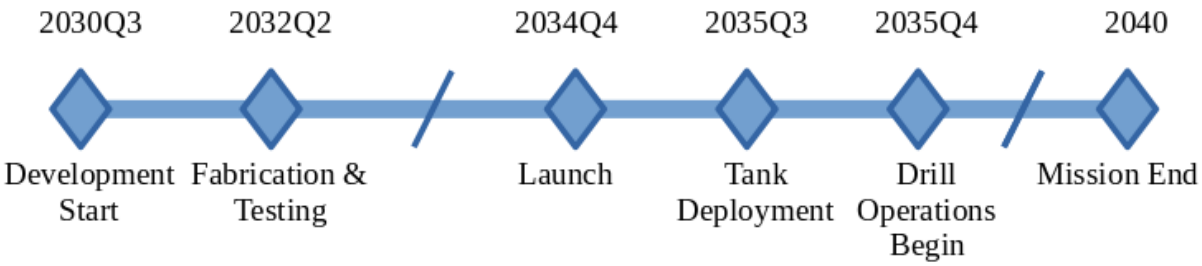

Figure 1: Mission timeline from development to end of mission.

2. Production of Fuel and Oxidizer

The goal of this mission is to produce liquid fuel such that future missions to Mars will only need to bring enough fuel to get to the planet's surface before refueling for a return flight to Earth. The propellant mixture currently showing the most progress is the roughly 3.5:1 ratio of O_2:CH_4, liquid oxygen to liquid methane because of the increased efficiency of methane as well as the ability to produce both propellant parts in-situ [20]. The creation of these two molecules comes from two separate reactions: water electrolysis and the Sabatier reaction. Electrolysis uses electrical current to split gaseous water into hydrogen (protons) and oxygen, the latter of which is stored for future fuel needs [21]. The protons are then used in the Sabatier reaction with atmospheric carbon dioxide to create methane and water [22]. Based on chemical equations, oxygen to methane production should be roughly 4:1 [23]; therefore, the requirements for fuel conversion are a feedstock of H_2O, a water electrolysis component, a feedstock of CO_2, and a Sabatier reactor component.

2.1 Current Practices

Current solutions suggest a two-step process: First, electrolysis uses polymer electrolyte membranes (PEM) to attain H_2 protons and O_2 from water followed by the Sabatier reaction to attain CH_4 and H_2O. PEM electrolysis has been the accepted next step in electrolysis due to its ability to operate within a large range of current densities and the thin proton-conducting membrane [21, 23]. The problem with this current solution is the large difference between the operating temperatures of PEM and the subsequent Sabatier reaction. PEM operates at roughly 80 ^{o}C whereas the Sabatier reaction operates closer to 300-400 ^{o}C. This difference requires two separately insulated and temperature-regulated systems which is an inefficient use of space, materials, and power. Our proposal, therefore, is to use an upscaled version of the Sabatier-Electrolyzer proposed by Nguyen et. al [24].

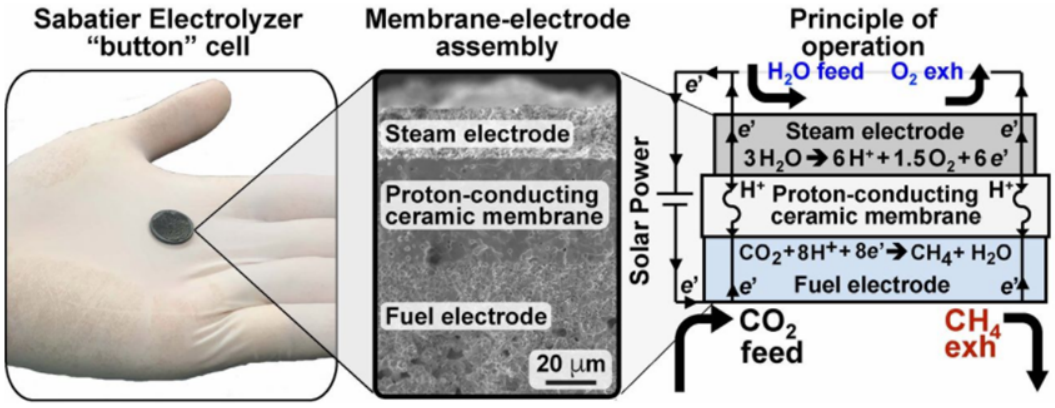

Figure 2: Image and description of a 'button' cell Sabatier-Electrolyzer as proposed by Nguyen et. al. The steam electrode facilitates water electrolysis, the proton-conducting ceramic membrane conducts protons from one reactor to the other, and the fuel electrode facilitates the Sabatier reaction. [24]

2.2 Sabatier-Electrolyzer Improved

Nguyen proposes using a replacement intermediator for PEM called proton-conducting ceramic membranes. Functionally, they act the same: behaving as an activation material for H_2O electrolysis and promoting subsequent migration of H protons across the membrane. The key difference is that protonic-ceramic electrolysis cells operate at much higher temperatures, ~400-600 ^oC, which is consistent with the 300-400 ^oC operation of the Sabatier reaction [23, 25]. The equivalence of operating temperature allows for the two reactions to be combined into one main reactor, reducing thermal regulation needs, overall complexity, and size of equipment. Additionally, the Sabatier equation generates roughly 164 kJ of energy per mole while the electrolysis of water requires an input of energy, though the amount is dependent on the current through the system and the environmental temperature of the system. If the electrical and thermal conditions are correctly balanced, however, it may be possible to create a thermo-neutral reactor which would greatly reduce total power consumption.

Nguyen has shown small-scale implementation of this combination in the form of a 'button' cell. As seen in Figure 2, both reactions are conveniently contained within a compact reactor requiring only a power source, feed line, and exhaust line. The entire system is then enclosed by an oven to ensure the temperature is maintained. Based on current testing, Nguyen estimates that a square meter of 10 cm x 10 cm cells could produce 4.728 gal-CH_4 / day. Given CH_4 is the limiting factor in these equations, since an O_2:CH_4 engine needs ~3.5:1 ratio and O_2 is made in excess at a rate of 4:1, the size of the cell bed would need to be roughly 2 m^2 [23, 24]. This size would require ~200 reactor cells in a combined array. With an encompassing oven and outer environmental shell, the reactor will be one of the larger project equipment pieces, but not by orders of magnitude. Therefore, as a contained system, this reactor saves large amounts of space, allowing other key mission projects to work with less stringent dimensional requirements.

Based on current work, the electrolyzer/Sabatier reactor has only been tested on a small scale 10 cm x 10 cm, but has shown promising thermal and efficiency results. However, given the AEGIR project will need a 200 cell combined reactor, which has only been tested in controlled, terrestrial laboratory environments, the system has a rough estimate of TRL 4. Further studies must be conducted to evaluate the system's endurance and robustness as well as how upscaling affects thermal and electrical balances.

3. Water Acquisition

The acquisition of water for electrolysis is done through a set of three mobile Rodriguez wells. At least one Rodwell will be operational at all times. The well locations are set by operators on Earth to maximize the usage of the underlying water table. Each well will produce 0.03 mT of water a day. Once inserted, the wells are kept stable by the casing used for the Rodriguez well shaft, allowing the solar panels to deploy without causing instability due to winds.

3.1 Rodriguez Wells

A Rodriguez well, or Rodwell, will be used to obtain water for the fuel production process. Rodwells have been used in analog operations on Earth, including at the South Pole station in Antarctica (TRL 6). The wells contain a shaft that leads to a bulb-shaped cavity in a subsurface ice sheet. Melt-water is pumped up the shaft to be used for surface operations [4]. The subsurface vertical profiles of the Martian Rodwell site are predicted to be comprised of a debris/sublimation till layer, which is a collection of rock and sedimentary material of varying size, a firn layer, which contains granulated snow and ice, and a solid ice layer. The Rodwell shaft will be driven through the debris and firn layers, and partially into the ice layer [5].

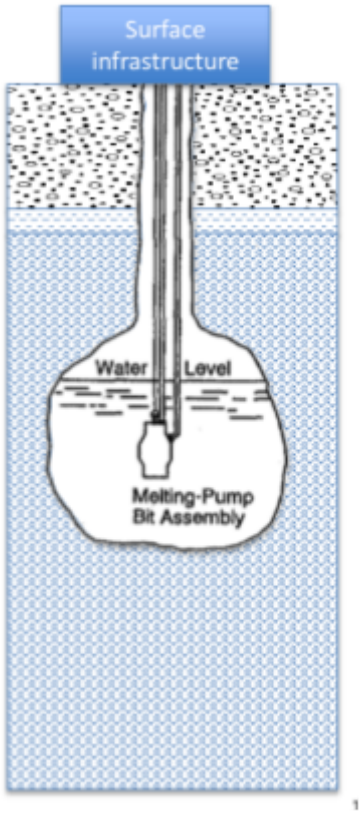

Figure 3: Diagram of a Rodriguez well setup with underground ice. [3]

To develop the wells, positions will be selected using ground-penetrating radar. A rotary-percussive mechanical drill will drive a hole through the debris layer [6]. This drill will be developed based on a scaled-up design of the Icebreaker drill, which has successfully demonstrated autonomous drilling, sample acquisition, and sample transfer in a Martian analog environment (TRL 6). In these analog studies, the Icebreaker drill has proven capable of drilling 1m deep in approximately 1 hour using ~100 W. This drill was selected for further development because of its ability to drill through multiple types of substrate (pure ice, ice-rich regolith, and whole rocks) and its relatively high TRL for drills capable of the required scale of drilling on the Martian surface. Since the predicted thickness of the debris layer is 0.5-10 m, the ground-penetrating radar will target sites with debris layer thicknesses that do not exceed drill capability [7][8]. The shaft drilled through the debris layer will be cased for stability. Casing the shaft of the Rodwell will also allow the well to be pressurized, which would mitigate water loss due to sublimation.

The firn layer is predicted to be negligible, but the well construction mechanism will be equipped with a hot water drill to add redundancy in the event that there is a firn layer of significant thickness [5]. Once a hole has been drilled into the ice, heat will be applied and the meltwater will pond. After sufficient reserve capacity has been established in the well, a submersible electric pump will be turned on and water will begin being pumped to the surface. The time allotted for well development, from initiation of drilling to full-functionality of the well, is one year. This is based on data from analog operations, predicted depth of the well, and considerations for drilling on Mars [9].

The size and shape of the well's ponding cavity and the amount of water in the reservoir at any time depend on the relative rates of water production via melt and water removal via both pumping and loss to surrounding (through sublimation or percolation). This dependency can be given by the equation:

$$\frac{\Delta m_w}{\Delta t} = \frac{[h_s(T_w - T_f) - q_s]}{l_e} - \frac{\Delta m_o}{\Delta t} - \frac{\Delta m_l}{\Delta t}$$

For the well function to remain stable, $\frac{\Delta m_w}{\Delta t}$, the change in water mass in the well, should equal zero [4].

3.2 Power and Mobility

Power for the wells is provided by two solar arrays with a combined surface area of 3 m^2, similar to the Insight lander. The panels are able to provide up to 5 kW when clean, reducing to 2.5 kW when obstructed due to dust [11]. Panels were chosen over RTGs due to the much higher potential daily power output of panels, and the primarily static nature of the wells mean that the size and mass downsides of panels are rarely a problem. Each well also has a large 2.4 kWh Lithium-ion battery, charged during the day by the solar panel. This battery is capable of fully absorbing the 2.5 kW from the solar panels.

Per-drill generation of 1,000 L of ice requires 140kWh total for the worst-case temperature of -80 to -100 ºC [3]. With 400 Wh for tank heating and 200 Wh for ancillary communication and filtering per day, the well has, at worst, 1.9 kWh available daily for melting and pumping operations. This corresponds to 73.35 days to acquire 1000 kg of water. This is, however, a power limit, and water table conditions are likely to reduce this rate over time as the well takes ice from the subsurface.

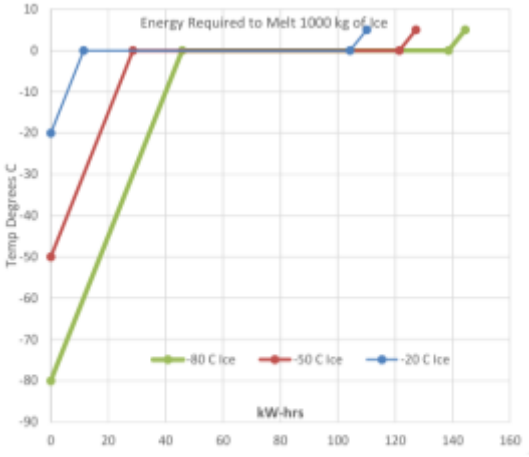

Figure 4: Energy requirements for melting underground ice into water at 5 C. [3]

During relocation, the solar panels will angle to 20 degrees from vertical to prevent wind from interfering with the now-detached drill. The relocation movement, combined with the steep angle, allow any dust accumulation to slip off to prevent excessive power loss. Before relocation, the drills spend one day without drilling, allowing the battery to charge up fully which powers the mobility system at 250 W for 10 hours, enough for traveling 500 meters. This value was derived by

assuming 100% of the mobility system power is being used for motion, and that the draw bar pull is equivalent to the weight of the drills.

The mobility system for the wells is a scaled-up version of the mobility system for the robots, capable of carrying the larger mass contained by the wells.

The wells are equipped with a camera for navigation for Earth operators to more easily navigate Mars, but more detailed maps of the area will be provided initially by the Mars Reconnaissance Orbiter and later on by LiDAR data acquired by the transportation robots. The low sensor and navigation capabilities of the wells was decided to simplify the electronics on the wells, especially due to the limited movement the wells can do compared to the robots due to a less mobile power system and higher mass.

4. Transportation

The transportation of water and drills is managed by a set of three robots, each capable of transporting 75 L of water from a drill to the chemical reactor. This transportation mechanism allows for more flexible placement of drills. The robots are also equipped with specific sensors, allowing accurate mapping of terrain. The robots are designed to be robust and scalable in order to function in a swarm-like configuration, managed by a central computer hosted on the central processing site. Robotic water transportation was chosen over laying fixed pipes, as the pipes potentially require robots for placement and the relatively low water output from the drill array negates the throughput benefit that pipes have.

4.1 Robot Design

Each robot is powered by an MMRTG (Multi-mission radioisotope thermal generator), equivalent to those on the Curiosity and Perseverance rovers. Each RTG is capable of generating 120 W at 30 V [12] on arrival, lowering to 90 W at the five-year mission end. The MMRTG is accompanied by a 1.2 kWh Lithium-ion battery, which is used to provide a higher possible power output during mission operations. The MMRTG allows for continuous excursions without returning to the processing plant and simplifies the electrical subsystem. A solar panel has a higher maximum power output, but provides no extra heat, is heavier, and the panel surface area needed could cause instability for the relatively low mass on the robot.

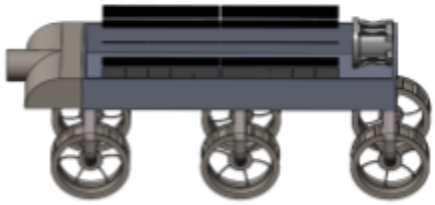

Figure 5: CAD Model of Transport Robot

At rest, the MMRTG provides 10 W to the onboard computer (a RAD750), as well as intermittent power to onboard communication systems. This results in 100 W available for charging or mobility, resulting in a charge time of 12 hours, increasing to 17 hours to full charge at mission end. Once charged, the combined output of the MMRTG and the battery allows a peak of 220 W for powering the mobility system for regular water transport operations for 10 hours. This decreases to 8 hours of regular operations or 3.6 hours at the end of the mission.

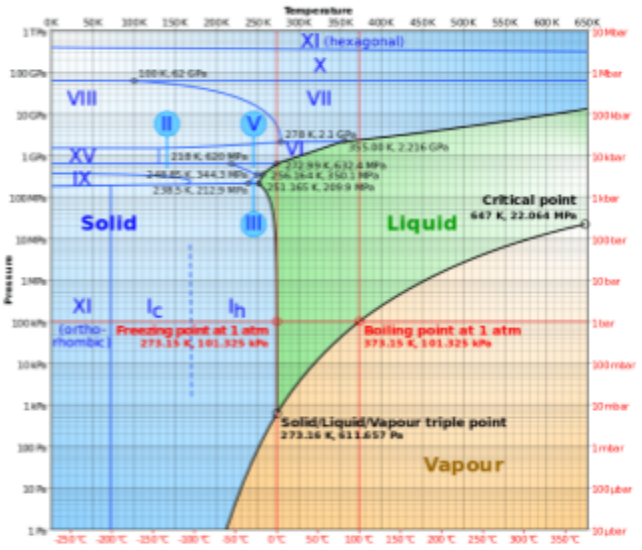

Figure 6: Phase transition diagram for water [14]

The fluid delivery system (FDS) is a tank on the robot which retrieves water from the Rodriguez wells and transports it to the central processing site, capable of storing 75 L. The FDS is initially at atmospheric Martian pressure at which liquid water rapidly evaporates, so the first tank's evaporation is used to pressurize the tank for future trips. The water in the tank is kept liquid by extending portions of the heatsink from the MMRTG into the FDS, extracting

about 100 W of the 2 kW [13] of thermal waste energy from the MMRTG into copper heating elements that extend into the bottom of the FDS. This is sufficient to keep a full tank of 75 L at 5 °C.

The FDS has a transfer port at the bottom rear of the tank, connected to a flexible hose with a magnetically charged tip for alignment. The tip is an inverted conical receptacle with a flat cover on top, designed to fit an equivalently shaped conical tip on the Rodriguez wells/CPS to stay covered from dust while traveling.

The wheel design is chosen to maximize pressure on the soil, increasing soil compaction to minimize shearing. The titanium struts from the robot's body to the wheels connect over the outside of the robot rather than the inside to prevent the robot from getting stuck on rocks. The wheel hub is connected to the external wheel by six titanium springs in order to reduce stresses due to sudden impacts with the terrain. The wheel rims around the grousers prevent the robot from slipping sideways on a slope [15]. These stability improvements are required to prevent sloshing of the tank, as well as to minimize the possibility of wheel damage.

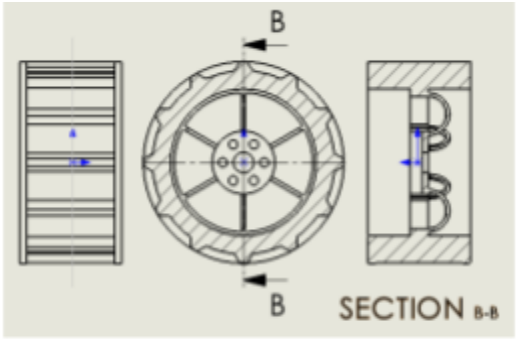

Figure 7: Technical Drawing of Rover Wheels

4.2 Navigation

The Swarm autonomy is necessary for the robots to avoid obstacles and each other, so when they carry out missions they are able to avoid collisions and possible redundancies. The Swarm uses a version of EKF-SLAM which allows for accurate readings in barren environments. The swarm is semi-autonomous as tasks can be assigned by "control" on earth, ensuring that the mission is operating as smoothly as possible. The sensors needed to run EKF-SLAM on the robot are LIDAR, an IMU, and an odometry sensor in the wheels; they are used to process the terrain moved through and for the robot to localize itself within a given map.

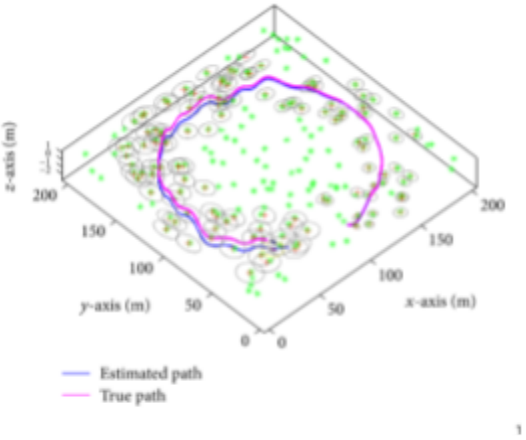

Figure 8: EKF-SLAM simulation. [18]

SLAM software allows for the robots to be able to traverse the Mars terrain. It will be used for robots to create a map that will identify obstacles in their path. However traditional SLAM is heavily dependent on finding discernible features in an area [17], but on Mars, there is no guarantee that there will be enough individual points to accurately build a map. To eliminate that issue the robots use EKF-SLAM which creates a stochastic map of vector stacking sensors and landmark states [16]. The map builds through sensor estimation of location and confirmation of landmarks. However, in the traditional EKF-SLAM algorithm the computational complexity and uncertainty grow rapidly with the increase of feature points and enlargement of map coverage. To make EKF-SLAM more computationally manageable and accurate for the robots in a barren environment like MARS, the robots are given predefined submaps. The EKF Algorithm can use the local submaps to localize the robot initially and when enough data is gathered to satisfy the interaction of the submap into the global map the robot can then localize itself within the entire map [18]. With the submodule maps the robots are able to create a more accurate map with much less computation, making it feasible for them to locally identify and avoid obstacles on the Mars terrain. EKF-SLAM has not been used on Mars but has been tested extensively on Earth, making it TRL-6.

5. Coordination

Tasking for the robot swarm and drills is managed in a centralized coordinator in the processing tank. This was chosen to simplify decision-making, as opposed to having the individual robots in the swarm determine their tasks and deal with conflicts [26]. The central coordinator is capable of assigning robots to extract water from wells and ordering wells to move between locations, with the well locations being set by operators on Earth. The coordinator is also responsible for managing entry into a region of 50m around the processing tank in which only one robot is allowed to drive at a given time. This is done on a first-come-first-serve system, where the robots request entry into the tank region and pause until their entry is accepted by the coordinator [19] (Fig 9). This is used to simplify the collision avoidance algorithms in the robots, as the large spacing of the wells means that collisions are only likely to occur around the processing tank drop-offs. The central coordinator is also used to transfer navigation and mapping information between the robots and wells and from the robots to Earth, allowing the wells to use maps created by robots for navigation and allowing Earth operators to better determine convenient well locations.

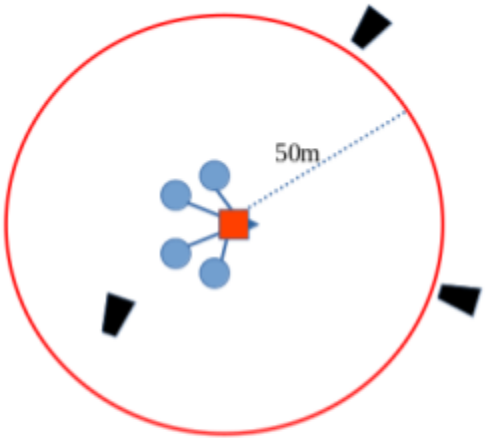

Figure 9: Diagram of the exclusion zone around the chemical reactor with one robot inside [19]

6. Storage

The storage system will have to store up to 11 T or 6,200 gallons of liquid CH_4 and 39 T or 8,200 gallons LOx for 1 year on the Martian surface before the cryogens are removed, and the system itself will need to last for at least 5 years without human maintenance. The cryogens will need to be stored separately and the cryogenic tanks will need mechanisms to control their internal pressures and temperatures to resist boil-off of cryogen and keep them thermodynamically stable at cryogenic temperature. There needs to be an input/output system for the tanks, and lastly, there needs to be consideration for how the tanks will be transported to Mars from Earth. If simply sending sufficiently large, rigid cryo tanks from Earth were done, there would be a significant waste of volume in the rockets due to the unused empty space inside of the tanks. Given that the purpose of this mission is to reduce space and mass used on round trip missions, it is relevant to the search for ways to improve packing efficiency in this design as well.

6.1 Container Design

A solution to improving packing efficiency would be to use inflatable “bladders” as the basis for the cryogenic tanks so that they could be collapsed in transit to Mars with no dead space. A flaw with inflatable tank designs is that the polymer materials used to make these experience increased brittleness and decreased flexibility at cryogenic temperatures. This process makes tank expansion with cryogens more difficult and causes microcracking in the polymer which damages its integrity. Recently research by Westra et al. has shown that this problem can be alleviated by folding the bladders into cylindrical origami structures [27]. They found that the geometries of these structures allowed polymers to be expanded and recompressed at least 100 times at cryogenic temperatures without experiencing microcracking. The optimal origami to use is the Kresling origami structure, due to other research finding it to have maximized compressibility and the minimal number of vertices which allow for points of failure, and for having a simple, one-dimensional deployment process, [28] as seen in figure 10.

The Kresling origami structure can then be applied to a design by Fleming and Thaxton for an inflatable tank to create the basis for a Liquid Origami Rigidized Drum (LORD) system [30]. There will be an inner “pressure” membrane and an outer “insulation” membrane that are held on a metal ring with legs and separated by a vacuum to minimize heat leak. Both membranes will be polymer Kresling

structures, and the pressure membrane will be suspended to the insulation membrane with epoxy struts. The bottom of the drum will be a metal cap that will support the weight of the system. The material of the pressure membrane should be Teflon FEP due to having superior permeability and decreased flammability compared to other polymers. The insulation material should be abrasion resistant to protect against dust storms, be resistant to UV radiation, and be an insulator. Kapton is a good candidate given these constraints. A resin will also be applied to the membranes that will cure and rigidify them when the material starts to reach cryogenic temperature [31]. A rigid container is more stable and less inclined to fall or collapse, and once the LORD systems have reached the Central Hub, the value of minimizing packing efficiency will no longer be necessary.

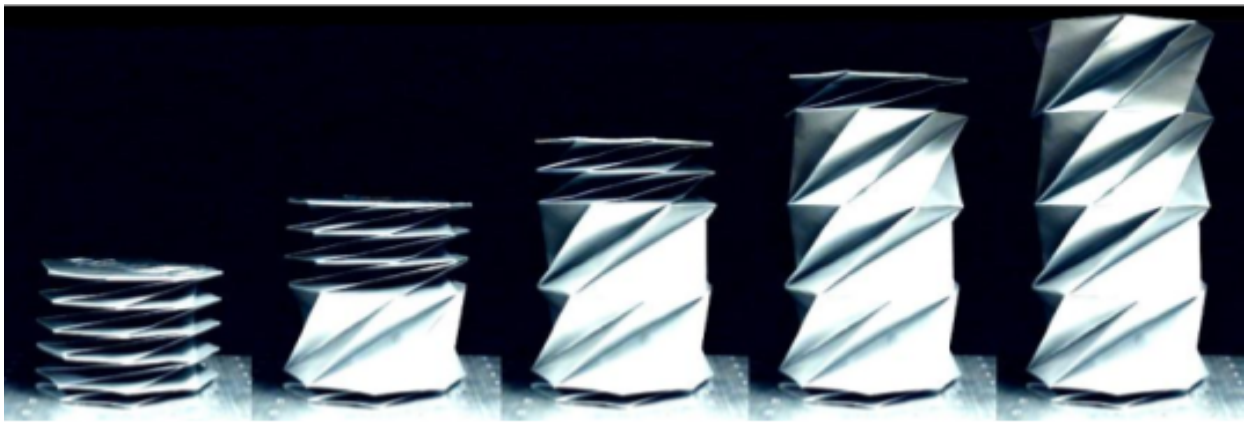

Figure 10: Proof of concept of Paper Kresling structure expanding [29]

Flexible piping equipped with Multi-Layer Insulation (MLI) will be placed on the top and bottom of the tank, connected straight through the pressure membrane. The piping can then be connected to the outlets of the Sabatier reactors and a Thermodynamic Venting System (TVS), the pressure and temperature regulation system for the LORD. Part of the pipe connections will also involve access to a pump for the robot swarm to control. The swarm can then top fill or bottom fill the tank as necessary for pressure regulation during the tank filling process.

6.2 Internal Regulation

The TVS is a set of two branches connected to the bottom and top of the tank that work in tandem with each other. The vented branch exposes the system to the outside and creates a cold source for a plated heat exchanger using a Joule-Thomson Valve, before releasing the vapor, which decreases the pressure in the tank. The injection loop pumps a mass fraction of liquid through the heat exchanger, subcooling it, before shooting it back through the top of the tank, which reduces stratification and temperature. The TVS activates as the pressure of the tank reaches a prescribed maximum and stops as it reaches a prescribed minimum [32]. Despite taking measures to decrease heat leak and boil off, it is impossible to completely eliminate it over the period required for storage, so the Sabatier reactors would effectively need to produce more than the minimum to have the required amount of propellant at year's-end.

Using Fleming and Thaxton's estimates and rounding up to include the piping and TVS, we estimate the total mass per tank to be around 600 kg. It should be noted that most of the mass comes from the metal support structure. Each tank should be capable of storing the minimum amount of LOx as well as having necessary ullage space for the vapor, so 9000 gal or 34.1 m^3 is a reasonable necessary max volume for the fully expanded tank. Using a found compressibility of 95.5% for a Kresling structure, the volume of a LORD at full compression in the rocket is 1.53 m^3. That number can be rounded up to 2 m^3 to estimate the volume of the entire system. Given that loss of ability to store at least of the cryogens would lead to mission failure, it is reasonable to take multiple backup LORDs, particularly given their light mass

and low compressed volume. Taking 4 drums, of which only 2 will be needed at a time, will take up 2400 kg or 2.4 T of mass and around 8 m^3 of volume on the rocket.

Several assumptions were made in this design. We assumed that the research done by Westra et al. can be easily scaled to large-scale systems such as the cryogenic tanks and that it could be applicable to other polymers than what was studied, which was BoPET. For mass and volume estimations, we assumed that the geometry of a fully compressed and fully expanded Kresling structure is similar enough to that of a right cylinder that we can approximate the volume of the former using the latter. We also assumed that the effects of the resin curing process won't have a significant effect on the integrity of the structure or material. Given the veracity of the assumptions made, we can not reasonably justify a TRL above 3 currently, but we are confident that the basis of the concept is solid and that given proper exploration of the design that number would see a quick rise in time for a proper mission.

7. Budget

The budget is based upon estimates from the Advanced Missions Cost Model [33], a machining quote for the robots [34], and several analogs such as NASA's InSight lander [35]. The final budget is estimated to be $6.61 billion. Future cost estimates will be calculated using NASA's Project Cost Estimating Capability (PCEC) software for more accurate estimates.

Item	Weight per Item (in tonnes)	Cost per Item (in millions)	Number of Items	Total Weight (in tonnes)	Total Cost (in millions)
Wells	4.8	700	3	14.4	2100
Robots	1.5	270	3	4.5	810
Converter	21	1800	1	21	1800
LORD Tanks	0.6	475	4	2.4	1900
Total				42.3	6610

Figure 11: Cost estimates for AEGIR [34, 35, 36]

8. Risk

Likelihood					
Certain					
Likely		[2]		[3]	
Possible			[8]	[1]	
Unlikely		[7]		[4], [9]	
Rare			[5]		[6]
Consequence	Negligible	Minor	Moderate	Critical	Catastrophic

1. Drill Damage
2. Well failure via freezing or depth increasing beyond power system capabilities.
3. Damage to solar panel
4. Motor failure that disrupts robot movement
5. Wheels don't account for terrain
6. Three out of four of the LORD systems rupture
7. Liquid boil-off rate is higher than expected
8. The efficiency of the processing bed is less than expected leading to increase water and CO2 input needs
9. Processing bed partially damaged
10. Processing bed destroyed or fails

9. Conclusion

In this paper, we have proposed Architecture for Extracting Groundwater In Regolith, a full solution for Mars-based ISRU for methalox propellant generation. AEGIR utilizes a distributed, scalable, and redundant architecture to acquire, transport, and generate the materials needed for cryogenic propellant. An ISRU of this scale would greatly facilitate sample return flights for autonomous Martian missions, and provide a stepping stone for human habitation. The technology required for the realization of AEGIR is not yet complete, but advancements in material science in the next decade will allow for a large and robust reactor framework to be launched with near-future spaceflight technology.

Appendix
Calculations

Liquid Propellent Needs:

- 50 Metric tons produced per year
- 3.5:1 O_2:CH_4
    - 38.89 MT O_2 : 11.11 MT CH_4

Conversion Calculations

- Predicted m^2 electrolysis/Sabatier cell bed CH_4 molar production = 4.728 gal/day
    - 1 m^3 = 0.984 MT = 264.2 gallons
    - 11.11 MT CH_4 ~ 3000 gal/year
- Assume 11 month production cycle
    - $\frac{3000\ gal}{335\ days}$ = 8.95 gal/day goal
    - $\frac{8.95}{4.728}$ ~ 2 m^2 cell bed

Citations

[1] L. Hall, "Overview: In-Situ Resource Utilization," *NASA*, Apr. 01, 2020. https://www.nasa.gov/isru/overview.

[2] A. M. Bramson, S. Byrne, N. E. Putzig, S. Sutton, J. J. Plaut, T. C. Brothers, and J. W. Holt, "Widespread excess ice in Arcadia Planitia, Mars," *Geophysical Research Letters*, vol. 42, no. 16, pp. 6566–6574, 2015.

[3] S. Hoffman, A. Andrews, and K. Watts, "'Mining' Water Ice on Mars An Assessment of ISRU Options in Support of Future Human Missions," 2016. [Online]. Available: https://www.nasa.gov/sites/default/files/atoms/files/mars_ice_drilling_assessment_v6_for_public_release.pdf.

[4] Lunardini, V. J., & Rand, J. (1995). Special Report 95-10 Thermal Design of an Antarctic Water Well.

[5] Hoffman, S., Andrews, A., & Watts, K. (2016). "Mining" Water Ice on Mars An Assessment of ISRU Options in Support of Future Human Missions.

[6] Horne, M. F. (2015). Drilling on Mars – Mathematical Model for Rotary-Ultrasonic Core Drilling of Brittle Materials. In UC Berkeley Electronic Theses and Dissertations (Vol. 13). https://escholarship.org/uc/item/6zg2x2d8

[7] Paulsen, G. and Zacny, K., "Mars Drilling: Development of a 1 m Class Rotary-Percussive Drill for Mars Permafrost", vol. 2019, 2019.

[8] Zacny, K., Paulsen, G., Chu, P., Mellerowicz, B., Yaggi, B., Klein-Henz, J., & Smith, J. (n.d.). The Icebreaker Drill System: Sample Acquisition and Delivery for the Lunar Resource Prospecting Mission.

[9] Hoffman, S. J., Lever, J. H., Andrews, A. D., & Watts, K. D. (2020). Mars Rodwell Experiment Final Report. http://www.sti.nasa.gov

[10] Lunardini, V. J., & Rand, J. (1995). Special Report 95-10 Thermal Design of an Antarctic Water Well.

[11]"Mars Surface Solar Arrays: Part 2 (Power Performance)," 2017. Accessed: Mar. 02, 2022. [Online]. Available: https://ntrs.nasa.gov/api/citations/20170006908/downloads/20170006908.pdf.

[12] "Multi-Mission Radioisotope Thermoelectric Generator (MMRTG)." [Online]. Available: https://mars.nasa.gov/internal_resources/788/.

[13] "National Aeronautics and Space Administration Multi-Mission Radioisotope Thermoelectric Generator (MMRTG)." [Online]. Available: https://mars.nasa.gov/mars2020/files/mep/MMRTG_FactSheet_update_10-2-13.pdf.

[14] Karla and O. C. Winter, "The when and where of water in the history of the universe," ResearchGate, Mar. 02, 2018. https://www.researchgate.net/publication/323507409_The_when_and_where_of_water_in_the_history_of_the_universe (accessed Mar. 02, 2022).

[15] B. M. D. Wills, "The Load Sinkage Equation in Theory and Practice," Proceedings of the Second International Conference on the International Society for Terrain-Vehicle Systems, pp. 199–246, Dec. 1966, doi: 10.3138/9781487584757-027.

[16] J. Solà, "Simultaneous localization and mapping with the extended Kalman filter 'A very quick guide... with Matlab code!,'" 2014. Accessed: Mar. 02, 2022. [Online]. Available: https://www.iri.upc.edu/people/jsola/JoanSola/objectes/curs_SLAM/SLAM2D/SLAM%20course.pdf.

[17] C. Thomson, "What is SLAM? (Simultaneous Localisation And Mapping)," *info.vercator.com*. https://info.vercator.com/blog/what-is-slam (accessed Mar. 02, 2022).

[18] B. Zheng and Z. Zhang, "An Improved EKF-SLAM for Mars Surface Exploration," *International Journal of Aerospace Engineering*, vol. 2019, pp. 1–9, Feb. 2019, doi: 10.1155/2019/7637469.

[19] Z. Yan, N. Jouandeau, and A. A. Cherif, "A Survey and Analysis of Multi-Robot Coordination," International Journal of Advanced Robotic Systems, vol. 10, no. 12, p. 399, Jan. 2013, doi: 10.5772/57313.

[20] "NASA Tests Methane Engine Components for Next Generation Landers | NASA." https://www.nasa.gov/centers/marshall/news/releases/2015/nasa-tests-methane-powered-engine-components-for-next-generation-landers.html (accessed Mar. 01, 2022).

[21] M. Carmo, D. L. Fritz, J. Mergel, and D. Stolten, "A comprehensive review on PEM water electrolysis," Int. J. Hydrogen Energy, vol. 38, no. 12, pp. 4901–4934, Apr. 2013, doi: 10.1016/J.IJHYDENE.2013.01.151.

[22] E. Moioli, N. Gallandat, and A. Züttel, "Model based determination of the optimal reactor concept for Sabatier reaction in small-scale applications over Ru/Al2O3," Chem. Eng. J., vol. 375, p. 121954, Nov. 2019, doi: 10.1016/J.CEJ.2019.121954.

[23] D. A. Nguyen, "Methane Synthesis Using a Sabatier-Electrolyzer Based on Proton-Conducting Ceramics," Colorado School of Mines, 2019.

[24] D. Nguyen, L. Q. Le, Z. Pan, G. S. Jackson, and N. P. Sullivan, "Making Fuel on Mars: Methane Synthesis from Martian-Derived CO2 and H2o Using a Sabatier Electrolyzer Based on Proton-Conducting Ceramics," ECS Meet. Abstr., vol. MA2019-02, no. 57, p. 2443, Sep. 2019, doi: 10.1149/MA2019-02/57/2443.

[25] T. Pritchard, R. J. Braun, and N. P. Sullivan, "Techno-Economic Analysis of the Sabatier Electrolyzer: CO2-to-Methane Using Proton-Conducting Ceramics," ECS Meet. Abstr., vol. MA2020-02, no. 40, p. 2657, Nov. 2020, doi: 10.1149/MA2020-02402657MTGABS.

[26] A. Anand, M. Nithya and T. Sudarshan, "Coordination of mobile robots with master-slave architecture for a service application," 2014 International Conference on Contemporary Computing and Informatics (IC3I), 2014, pp. 539-543, doi: 10.1109/IC3I.2014.7019647.

[27] K. Westra, F. Dunne, S. Kulsa, M. Hunt, and J. Leachman, "Compliant polymer origami bellows in cryogenics," *Cryogenics*, vol. 114, Mar. 2021.

[28] J. Butler, J. Morgan, N. Pehrson, K. Tolman, T. Bateman, S. P. Magleby, and L. L. Howell, "Highly compressible origami bellows for Harsh Environments," *40th Mechanisms and Robotics Conference*, vol. 5, Dec. 2016.

[29] N. Kidambi and K. W. Wang, "Dynamics of kresling origami deployment," *Physical Review E*, vol. 101, no. 6, 2020.

[30] D. C. Fleming and E. A. Thaxton, "Evaluation of Design Concepts for Collapsible Cryogenic Storage," *2001 NASA/ASEE SUMMER FACULTY FELLOWSHIP*, pp. 53–62, 2001.

[31] R. E. Freeland, G. D. Bilyeu, and M. M. Mikulas, "Inflatable Deployable Space Structures Technology Summary," *L'Garde*, Sep. 28, 1998. https://mars.nasa.gov/mars2020/files/mep/MMRTG_FactSheet_update_10-2-13.pdf.

[32] S. Mer, D. Fernandez, J.-P. Thibault, and C. Corre, “Optimal design of a Thermodynamic Vent System for cryogenic propellant storage,” *Cryogenics*, vol. 80, pp. 127–137, Dec. 2016, doi: 10.1016/j.cryogenics.2016.09.012.

[33] A. Owens and O. de Weck, "Sensitivity Analysis of the Advanced Missions Cost Model," in *46th International Conference on Environmental Systems*, Vienna, Austria, 2016.

[34] mars.nasa.gov, “NASA’s InSight Mars Lander,” *NASA’s InSight Mars Lander*, 2019. https://mars.nasa.gov/insight/.

[35] “CNC Machining Services,” *Xometry*. [Online]. Available: https://www.xometry.com/?utm_term=xometry&utm_campaign=PB:G%7CNT:SN%7CAN:Manufacturing%7CCN:Branded&utm_source=adwords&utm_medium=ppc&hsa_acc=3789459769&hsa_cam=608070446&hsa_grp=67613041575&hsa_ad=405818908935&hsa_src=g&hsa_tgt=kwd-297018084385&hsa_kw=xometry&hsa_mt=e&hsa_net=adwords&hsa_ver=3&gclid=CjwKCAiApfeQBhAUEiwA7K_UH9EREqpxN-yaU8on_yrW1oqYIL2enCDtWdw2Awwa92Lz9XZz_dexCRoCTf8QAvD_BwE

[36] J. E. Werner, S. G. Johnson, C. C. Dwight, and K. L. Lively, “Cost comparison in 2015 dollars for radioisotope power systems -- Cassini and Mars Science Laboratory,” *Cost Comparison in 2015 Dollars for Radioisotope Power Systems -- Cassini and Mars Science Laboratory (Technical Report) | OSTI.GOV*, 01-Jul-2016. [Online]. Available: https://www.osti.gov/biblio/1364515. [Accessed: 02-Mar-2022].